

The Diverse Stellar Populations of the W3 Star Forming Complex

Eric D. Feigelson and Leisa K. Townsley

*Department of Astronomy and Astrophysics, Pennsylvania State University, 525 Davey
Laboratory, University Park, PA 16802*

edf@astro.psu.edu

ABSTRACT

An ~ 800 arcmin² mosaic image of the W3 star forming complex obtained with the *Chandra X-ray Observatory* gives a valuable new view of the spatial structure of its young stellar populations. The *Chandra* image reveals ~ 1300 faint X-ray sources, most of which are PMS stars in the cloud. Some, but not all, of the high-mass stars producing hypercompact and ultracompact HII (UCHII) regions are also seen, as reported in a previous study.

The *Chandra* images reveal three dramatically different embedded stellar populations. The W3 Main cluster extends over 7 pc with ~ 900 X-ray stars in a nearly-spherical distribution centered on the well-studied UCHII regions and high-mass protostars. The cluster surrounding the prototypical UCHII region W3(OH) shows a much smaller (≤ 0.6 pc), asymmetrical, and clumpy distribution of ~ 50 PMS stars. The massive star ionizing the W3 North HII region is completely isolated without any accompanying PMS stars. In W3 Main, the inferred ages of the widely distributed PMS stars are significantly older than the inferred ages of the central OB stars illuminating the UCHIIs. We suggest that different formation mechanisms are necessary to explain the diversity of the W3 stellar populations: cluster-wide gravitational collapse with delayed OB star formation in W3 Main, collect-and-collapse triggering by shock fronts in W3(OH), and a runaway O star or isolated massive star formation in W3 North.

Subject headings: stars: formation – stars: pre-main sequence – ISM: clouds – ISM: individual (Westerhout 3) – open clusters and associations: general – X-rays: stars

1. Introduction

W3 (Westerhout 3) is perhaps the most active region of current star formation in the nearby Galaxy. Extending 30 pc along the edge of a $M \simeq 5 \times 10^4 M_\odot$ giant molecular cloud (GMC), the star-forming complex has dozens of embedded young massive stars producing a variety of pre-stellar condensations, hot molecular cores, hypercompact to small HII regions, maser clusters, and molecular outflows (e.g., Lada et al. 1978; Reid et al. 1980; Dreher & Welch 1981; Tieftrunk et al. 1997; Chen et al. 2006). Its infrared sources have an integrated luminosity of several $\times 10^5 L_\odot$. Situated just east of W3 are the older IC 1795 and IC 1805 clusters, the latter lying within the enormous W4 superbubble/chimney structure blown by generations of massive stars. The W4–IC 1795–W3 complex is widely considered to be an exemplar of sequential triggered star formation (Lada et al. 1978; Oey et al. 2005). Recent SCUBA observations of the W3 GMC find a higher percentage of the gas mass gathered into dense molecular clumps at the eastern edge compared to the undisturbed parts of the W3 GMC, supporting this triggering scenario (Moore et al. 2007). A detailed description of the W3 and W4 complexes and a thorough review of the literature are given by Megeath et al. (2007).

The richest site of massive star formation in W3 is the W3 Main cluster of embedded OB stars, dominated by the very young and luminous IRS 4 and IRS 5 sources. IRS 5 lies at the center of a 0.1 pc concentration of massive stars resembling a nascent counterpart of the Orion Trapezium (Megeath et al. 2005). W3(OH) to the southeast and W3 North to the north have massive stars but appear less active than W3 Main. The distance to the complex is accurately measured from maser kinematics to be 2.0 kpc (Xu et al. 2006; Hachisuka et al. 2006).

Despite the intense study of W3 at radio, millimeter, and infrared wavelengths, little is known about its low mass stellar population. For example, a *JHK* near-infrared (NIR) survey of $5' \times 5'$ in W3 Main reveals ~ 40 sources with *K*-band excesses indicative of Class I–II pre-main sequence (PMS) stars with disks (Ojha et al. 2004). Hundreds of other stars are detected, but infrared photometry cannot discriminate disk-free Class III PMS stars from the strongly contaminating population of unrelated Galactic field stars (mostly red giants). A new mid-infrared (MIR) photometric survey of W3 Main, IC 1795, and W3(OH) with the *Spitzer Space Telescope* helps to identify cluster members (Ruch et al. 2007), but it suffers confusion from three effects: foreground and background Galactic field stars (Benjamin et al. 2005), bright diffuse emission produced by heated dust around the HII regions (Povich et al. 2007), and extragalactic objects with MIR excesses (Harvey et al. 2007).

X-ray surveys of young stellar clusters (YSCs) with the *Chandra X-ray Observatory* are surprisingly efficient at detecting low mass PMS populations, even at distances around

2 kpc and at obscurations $10 < A_V < 150$ mag typical for W3 stars. PMS X-ray emission arises primarily from violent magnetic reconnection events, similar to solar flares but far more powerful, and is largely independent of circumstellar disks or accretion (see reviews by Feigelson & Montmerle 1999; Feigelson et al. 2007). Luminous and spectrally hard X-ray flares are present throughout the PMS phases of Class I–II–III at levels $10^2 - 10^3$ above that seen in old disk populations (Preibisch & Feigelson 2005), so relatively few Galactic disk interlopers appear in X-ray samples. These field star X-ray sources and extragalactic contaminants are easily removed (Getman et al. 2006). Due to a poorly-understood statistical association between X-ray luminosity and PMS stellar mass (Preibisch et al. 2005; Güdel et al. 2007), a flux-limited X-ray observation of a young stellar cluster will be roughly complete down to a corresponding mass limit.

Taking together these properties of X-ray studies, we find that X-ray surveys at sufficiently high spatial resolution and sensitivity provide uniquely rich, largely disk-unbiased, mass-limited, and nearly uncontaminated samples of PMS stars in both embedded and unobscured YSCs. These samples complement MIR surveys obtained with the *Spitzer Space Telescope*, which generally extend down to lower masses (including the brown dwarf regime) but cannot readily discriminate disk-free PMS stars from field stars. *Spitzer* thus detects more diskless Class 0-I-II systems while *Chandra* effectively samples Class III systems in addition to many Class I and II stars. The X-ray samples are useful for various astrophysical purposes such as probing the stellar Initial Mass Function, protoplanetary disk evolution, and magnetic activity.

In an early *Chandra* study, two ~ 20 ks exposures of a ~ 300 arcmin² field in W3 Main revealed 236 X-ray sources (Hofner et al. 2002). Several are associated with massive stars ionizing HII regions but most do not have counterparts in *JHK* images. We report here an extension of those efforts with a *Chandra* mosaic of 7 exposures totaling ~ 230 ks over ~ 800 arcmin², spanning much of the W3 star forming complex (Figure 1). A preliminary discussion of this mosaic, a *Chandra* Large Project, is given by Townsley (2006). Over 1300 X-ray sources are seen; a full listing and study of their properties will be presented in a separate paper. For each source, *Chandra* observations provide a sub-arcsecond position, line-of-sight absorption, and rough mass estimate in addition to magnetic activity characteristics.

We discuss here insights into the global structure and origins of the W3 stellar populations derived from the new *Chandra* data. The brief presentation of the observations in §2 will be expanded in a forthcoming paper with complete source lists similar to our group’s recent studies of the Cep OB3b (Getman et al. 2006), Pismis 24 (Wang et al. 2007a), M 17 (Broos et al. 2007), RCW 49 (Tsujiimoto et al. 2007), and Rosette star forming region (Wang et al. 2007b,c) YSCs. The three well-studied star forming regions in W3 are described

and contrasted in §3, and explanations for their origin are considered in §4. Section 5 considers in more detail the implications of the W3 Main results for astrophysical models of star cluster formation.

2. Observations and data reduction

The X-ray observations were made with the Advanced CCD Imaging Spectrometer (ACIS) camera on board the *Chandra X-ray Observatory* (Weisskopf et al. 2002). Three contiguous regions of the W3 star forming complex were observed with the $17' \times 17'$ ACIS imaging array (ACIS-I) for roughly 80 ks each, divided into seven exposures: three on W3 Main, one on W3(OH), and three on W3 North. Except for the two ~ 20 -ks W3 Main exposures discussed by Hofner et al. (2002), all were obtained between January and November 2005.

Data analysis followed procedures described in our group’s previous ACIS studies of young stellar clusters (e.g., Townsley et al. 2003; Getman et al. 2005; Wang et al. 2007a; Broos et al. 2007). X-ray events were corrected for CCD charge transfer inefficiency (Townsley et al. 2002) and the data were cleaned in a variety of ways (Townsley et al. 2003). The event data were corrected to the *Hipparcos* reference frame by alignment of bright on-axis X-ray sources with 2MASS stars then registered to a common astrometric reference frame based on *Chandra* boresights. A preliminary source list was identified from the merged observations using a wavelet-based algorithm (Freeman et al. 2002). Individual positions are generally accurate to $\pm 0.4''$ and double sources can be resolved at separations $\gtrsim 0.7''$. Images were created in soft (0.5–2 keV) and hard (2–7 keV) bands and were corrected for exposure variations, then adaptively smoothed using the CIAO tool *csmooth* (Ebeling et al. 2006) to make the mosaic shown in Figure 1.

3. The X-ray stellar populations in W3

3.1. W3 Main

W3 Main is a massive YSC, famous for containing every known type of radio HII region from hypercompact to diffuse, 0.01 to 1 pc in diameter, with ages 10^3 – 10^6 yrs (Tieftrunk et al. 1997). These HII regions are embedded in a complex, highly clumped molecular environment, with the younger (smaller) regions associated with the densest clumps (Megeath et al. 2007, and references therein). Most radio and NIR studies have concentrated on the dense central regions of the cluster, hence the complex was described as

only $\sim 4'$ in size (Tieftrunk et al. 1997).

Figure 2 shows this central region of the W3 Main cluster in the mosaicked *Chandra* image. X-ray point sources in our preliminary source list are marked with blue circles; additional faint X-ray sources are likely to emerge in our complete analysis, which will involve image reconstructions of crowded regions (Townsend et al. 2006). The radio HII regions detailed in Tieftrunk et al. (1997) are shown schematically as magenta ovals. X-ray sources that match the bright infrared sources from Table 1 of Ojha et al. (2004) are marked with green circles and labeled. Six of these sources were found in the earlier *Chandra* study of this region (Hofner et al. 2002). Two sources in the IRS5 region match NIR sources in Table 1 of Megeath et al. (2005) and are labeled using their nomenclature.

The wide-field *Chandra* mosaic (Figure 1) shows that the W3 Main YSC extends well beyond this central region; it is rich and roughly spherical, resembling the clusters that dominate many massive star forming regions. Its full extent is quite large; over 900 X-ray sources are distributed over the $17'$ (10 pc) ACIS-I field centered around $(\alpha, \delta) = (02:25:41, +62:05.9)$ close to W3 IRS5. The cluster is so large that for some stars, it is difficult to distinguish membership in W3 Main from membership in the less absorbed IC 1795 cluster to the southeast. Figure 3 shows how the dense concentration of lower mass stars in the inner $\sim 1'$ centered around IRS 5, known from earlier NIR observations (Megeath et al. 1996; Tieftrunk et al. 1998; Ojha et al. 2004), extends smoothly with the stellar surface density decreasing a factor of ~ 300 out to a radius of $5'$ (3 pc). When the X-ray luminosity function is corrected for contaminating sources and limited sensitivity, and then scaled to the well-characterized Orion Nebula Cluster (e.g. Wang et al. 2007a), the inferred cluster population will be several thousand stars. The stellar distribution in the central region is nearly but not entirely symmetrical; an excess of stars is seen $\sim 1'$ NW of IRS 5 around the W3 D and W3 H UCHIIs compared to a symmetrical region SE of IRS 5 where no massive stars are present.

The finding we emphasize here is not the previously known concentration of high mass stars in the cluster core but the richness, extent, and symmetrical appearance of the W3 Main stellar cluster on scales of several parsecs. The vast majority of these sources are low-mass PMS stars with only minor contamination by Galactic field stars or extragalactic sources (e.g. Wang et al. 2007a). While the stellar concentration in the central portion can be seen in *K*-band images (Megeath et al. 1996; Tieftrunk et al. 1998; Ojha et al. 2004), the full extent and simple structure of W3 Main cannot be discerned in the NIR due to the combination of patchy obscuration, nebular emission, and Galactic field star contamination.

3.2. W3(OH)

W3(OH) is a rapidly developing UCHII region, seen in the radio as an expanding shell of dense ionized gas around a heavily obscured ($A_V \sim 50$) late-O star (Dreher & Welch 1981; Turner & Welch 1984). The expansion age is $\sim 2 \times 10^3$ yr although an astrochemical model of the molecular species suggests an age around $10^4 - 10^5$ yr (Kawamura & Masson 1998; Kim et al. 2006). Six arcseconds east of W3(OH) lies the molecular hot core W3(H₂O) with three radio continuum peaks, maser emission, and an unusual radio synchrotron jet (Wyrowski et al. 1999, and references therein). This small complex is sometimes called the Turner-Welch Object. In a NIR image with $K < 17.5$, a stellar cluster with ~ 200 stars is seen with an elongated $\sim 1'$ distribution around the UCHII region; this is the one of the richest groupings of NIR stars within the huge W3/W4/W5 star forming complex (Tieftrunk et al. 1998; Carpenter et al. 2000). NIR data also reveal two smaller clusters northeast of W3(OH) (Tieftrunk et al. 1998).

The *Chandra* image shows that the YSC surrounding W3(OH) is much smaller, sparser, and less symmetrical than W3 Main (Figure 4). About 50 absorbed X-ray stars lie in a region $0.5 \times 1'$ (0.3×0.6 pc) oriented NE–SW around W3(OH). This cluster is accompanied by two sparse clumps with about 5 and 20 stars, respectively, lying $\sim 0.5 - 1.5$ pc to the NE of W3(OH), cospatial with small clusters seen in earlier NIR studies (Tieftrunk et al. 1998).

The young massive star ionizing W3(OH) is clearly detected in our *Chandra* observation, at (02:27:03.84, +61:52:24.9). It is a surprisingly hard X-ray source; this hard emission allows it to be seen through a large absorbing column ($A_V \sim 75$ mag) inferred from the soft X-ray absorption. The nearby high-mass system W3(H₂O), likely powered by a protobinary of early-B stars (Chen et al. 2006), is undetected in our X-ray data.

3.3. W3 North

The bright HII region G133.8+1.4 = W3 North is less well-studied than the regions considered above. The nebula is excited by an optically visible O6 star, #102 in the study of IC 1795 by Ogura & Ishida (1976) and #7044 in the study by Oey et al. (2005). It lies in a molecular cloud environment with density ~ 600 cm⁻³ and mass $\sim 230 M_\odot$, more than an order of magnitude below values for W3 Main and W3(OH) (Thronson et al. 1984, 1985). The ionized nebula is as bright as W3 A near IRS 5 in W3 Main; it has a diameter of $2'$ with estimated age $\sim 10^5$ yr (van der Werf & Goss 1990).

We clearly detect the O6 star in our *Chandra* observation, at (02:26:49.62, +62:15:35.0). However the *Chandra* source distribution around this O star differs dramatically from that

seen in either W3 Main or W3(OH): no cluster of PMS stars is found in its vicinity (Figure 5). The nearest X-ray source is $> 35''$ distant and the local source density is consistent with the general level of distributed young stars and contaminants seen $5' - 10'$ away. The absence of a cluster in W3 North was suggested by Carpenter et al. (2000) based on NIR imagery, and we strongly confirm this result with our X-ray observations.

4. Interpreting population differences

We find that three famous massive star-forming sites in the W3 cloud show remarkable variety in their low mass stellar distributions: a rich spherical cluster, an elongated collection of sparse star clumps, and a completely isolated O star. Evidence for these differences was provided by earlier infrared studies, but the *Chandra* dataset gives a more definitive view of this morphological diversity from its more complete and unbiased sample of the low mass population. We can discuss the origin of the structures in W3.

The W3(OH) cluster is an order of magnitude smaller and roughly 20 times less rich than the W3 Main cluster. The patchy distribution of stars, elongated along an axis perpendicular to a vector pointing towards the older IC 1795 cluster, supports a triggered origin due to IC 1795 ionization and wind shock fronts as discussed by Oey et al. (2005). The two small clusters, seen both in NIR (Tieftrunk et al. 1998) and X-ray images, lie along this same line and could have been triggered by the same shocks. The morphology of the PMS stellar distribution around W3(OH) resembles those seen in small cometary globules (Sugitani et al. 1995; Getman et al. 2007) and in larger molecular clouds (Zavagno et al. 2006; Deharveng et al. 2006; Broos et al. 2007) at the edges of HII regions. The elongation in stars around W3(OH) appears perpendicular to the axis pointing towards IC 1795, similar to the elongation of the M17 SW stellar distribution which lies along the photodissociation region and perpendicular to the axis pointing towards the M17 central cluster NGC 6618 (Broos et al. 2007). The W3(OH) structure has the fragmented and elongated appearance expected from the “collect and collapse” scenario of triggered star formation at the edge of an HII region (Elmegreen & Lada 1977; Whitworth et al. 1994; Dale et al. 2007).

For W3 North, we have a clear demonstration that its ionizing O star is isolated, unaccompanied by a cluster of lower mass stars. The simplest explanation is a runaway O star ejected from a rich cluster in the W3/W4 region. The W3 North radio continuum structure does have a cometary tail on the SSE side of the ionizing star, suggesting a northwesterly motion through the molecular medium (van der Werf & Goss 1990). This is inconsistent with an origin in W3 Main which would require a northeasterly motion, but may indicate an origin in the older IC 1795 or IC 1805 clusters. Accurate proper motions are needed to

test this model¹.

An alternative explanation, which seems feasible although improbable, is an origin within the local W3 North molecular cloud. Statistical simulations of sparse clusters with random draws from a standard Initial Mass Function show a wide dispersion of maximum stellar masses (Bonnell & Clarke 1999) and a few cases of field O stars support occasional formation of massive stars in isolation (de Wit et al. 2005). In particular, the late-O star ionizing KR 140, lying a degree south of W3 Main in the W3 molecular cloud, may have formed in isolation (Ballantyne et al. 2000).

Our findings do not support a simple unified origin of W3 North, W3 Main, and W3(OH) as proposed by Oey et al. (2005). In their interpretation, the three regions of high-mass star formation are components of a shell of molecular cloud material triggered into gravitational collapse by the ionization and wind shocks produced by the older IC 1795 star cluster lying east of the W3 molecular cloud. In contrast, we find that only the W3(OH) stellar population has the morphology expected from direct triggering by IC 1795 shock fronts. The other two W3 stellar populations have very different morphologies: the single O star ionizing W3 North either formed in isolation or was dynamically ejected from one of the richer nearby clusters, and the W3 Main cluster has a spherical, centrally condensed appearance that does not reflect the recent passage of a shock.

5. The origin of the W3 Main cluster

5.1. Two critical properties of W3 Main

Two inferences can be made from the morphology shown in Figure 3. These provide strong constraints on the formation process of the rich W3 Main cluster.

First, as outlined above and shown in Figure 3, the large-scale sphericity of the cluster implies that the role of triggering by shocks from the older IC 1795 cluster (or by the W4 superbubble further to the east) discussed by Oey et al. (2005) is negligible, or at most indirect, in the sense that the star formation did not follow the passage of a localized shock. There is no elongation of the stellar distribution along an East-West axis associated with a shock.

¹The NOMAD catalog (Zacharias et al. 2005) reports very large proper motions (~ 200 mas yr⁻¹) for this star based on photographic sky survey plates, but examination of the Digitized Sky Survey using NASA’s *SkyView* service shows a bright source in the same location in both DSS1 and DSS2, implying that the NOMAD proper motions are erroneous. The region has bright irregular nebular emission, so mistakes can easily be made.

W3 Main was either formed independently of an external trigger, or has dynamically evolved so that evidence of its triggered origin has been erased. The centrally concentrated, spherical morphology resembles the distribution of X-ray stars in the Orion Nebula Cluster ionizing the Orion Nebula (Feigelson et al. 2005), the NGC 6618 cluster ionizing the M 17 HII region (Broos et al. 2007), the NGC 2244 cluster ionizing the Rosette Nebula (Wang et al. 2007b), and many other YSCs. These stand in contrast to the unconcentrated and elongated stellar distributions attributable to shock triggering in small cometary globules (Sugitani et al. 1995; Getman et al. 2007; Ogura et al. 2007) and in larger molecular clouds (Zavagno et al. 2006; Deharveng et al. 2006; Broos et al. 2007) at the edges of HII regions.

The second inference concerning the origin of W3 Main to be made from the *Chandra* image is that at least some of the OB stars—those ionizing the well-studied hypercompact and ultracompact HII regions at the core of W3 Main—formed after the bulk of the more widely distributed cluster PMS stars. These HII regions have dynamical ages of $10^3 - 10^5$ yr (Tieftrunk et al. 1997)². If the PMS stars had similar ages, they would all be Class 0–I protostars.

However, only a few percent of ACIS sources are Class II, and $< 1\%$ appear to be Class 0–I in the Ruch et al. (2007) dataset of the brighter *Spitzer* sources. It is not possible that there exists a vast population of Class 0–I sources undetected by *Spitzer* in the outer regions of W3 Main. In the central region around IRS 5, where *Spitzer* sensitivity is limited by the bright diffuse emission, Megeath et al. (1996) found that no more than 30% of the NIR sources were Class I. This implies that most of the PMS stars in W3 Main are Class III, as in most other young stellar clusters observed with *Chandra*, and the age of the low-mass population is > 0.5 Myr. Even in clusters rich in Class 0 protostars, such as NGC 1333, many X-ray sources are Class II and III systems (Getman et al. 2002). This discrepancy in W3 Main may constitute the best case that a PMS population is much older (> 0.5 Myr) than at least part of its associated OB population (< 0.1 Myr).

If the PMS stars are characteristically 10^6 years old and some of the central OB stars are $< 10^5$ years old, those OB stars must have formed after the lower mass stars. This form of age spread has long been noted in older stellar clusters from studies of HR diagrams (Herbst & Miller 1982; Adams et al. 1983; Doom et al. 1985; Shull & Saken 1995; DeGioia-Eastwood et al. 2001). A young age has also been indirectly suggested for the

²Under special circumstances, an HII region can appear as an UCHII at later times (Franco et al. 2007). This requires either that the O star is nearly stationary ($\ll 1$ km s⁻¹ motion) at the center of a dense molecular core, or that it has entered a second core at a later time. It seems doubtful that this would fortuitously occur for several O stars in the central region of W3, and in any case can not explain the hypercompact regions in W3 M.

Trapezium OB stars in Orion based on the inferred short lifetimes of proplyds in the presence of ultraviolet photoevaporation (O’Dell 1998). The W3 Main OB stars are directly confirmed to be extremely young and still forming based on their very small HII regions; this is crucial for establishing that the central OB stars formed after the larger PMS population.

5.2. Implications for the formation of W3 Main

Together, these two results strongly preclude the application of an old and simple model of cluster and high mass star formation (see reviews by Bonnell et al. 2007 and Larson 2007). Pre-stellar molecular cloud condensations were traditionally thought to be centrally concentrated with higher densities ρ at the center; e.g., an isothermal equilibrium Bonnor-Ebert sphere. The free-fall time is then shorter at the core, $t_{ff} \propto \rho^{-1/2}$, implying rapid gravitational collapse and fragmentation. Gas quickly falls into the central region where, if Bondi-Hoyle accretion is unimpeded, the more massive protostars tend to grow fastest according to $\dot{M} \propto M^2$. Disk accretion of high mass protostars can be very rapid with $\dot{M} \sim 10^{-4} M_{\odot} \text{ yr}^{-1}$ implying full growth in $\sim 10^5$ yr (see review by Cesaroni et al. 2007). In these simple scenarios for cluster formation, OB stars concentrated in the cores might be older, but certainly not younger, than the surrounding lower mass PMS stars.

However, several more complicated models for cluster and high-mass star formation are consistent with our W3 Main results:

1. Star formation in large molecular clouds may occur inefficiently over a prolonged period, perhaps because their dynamics are dominated by supersonic turbulence within which only a small fraction of the molecular material resides in dense cores at a given moment (Tan et al. 2006; Krumholz & Tan 2007). The bulk of the stars may form in a quick burst of star formation at the end of the cloud’s life, as the star formation rate becomes efficient only when turbulence has subsided and the cloud contracts (Palla & Stahler 2000). Astrophysical issues relating slow and fast star formation in clusters are discussed by Elmegreen (2007). W3 Main exhibits a particular mass-dependency in its extended star formation history in that the majority of lower mass stars appear in the widely distributed older population while only a minority accompany the OB stars at the core.
2. The formation of massive OB stars specifically might be delayed with respect to lower mass stars. This delay might occur during the gaseous phase, where the formation of a high density core may be inhibited by the combined effect of many protostellar

outflows (Li & Nakamura 2004). Or the delay might occur during the stellar dynamical phase, waiting for stars to settle into the core gravitational potential where mergers form massive stars (Bonnell et al. 1998).

3. Star formation may occur primarily in spatially distributed molecular cores which, only after forming many lower mass stars over an extended time, settle towards the cluster center where densities are sufficiently high to form high-mass stars. A version of this model is described by McMillan et al. (2007) as an explanation for mass segregation in massive clusters.
4. W3 Main may contain two generations of OB stars, the latter arising from triggering by the growing HII regions of the former (Tieftrunk et al. 1997). The basis for this model is the presence of both diffuse HII regions (W3 A, D, H, J, and K in Figure 2) and ultracompact and hypercompact HII regions (W3 B, E, F, G, and M). This would be a case of internal triggering by W3 OB shocks rather than external triggering by IC 1795 shocks.

At present, we cannot differentiate between these models for W3 Main. A useful observation would be high spatial resolution MIR imaging to study disk properties of the lower mass *Chandra* stars in the close vicinity of the OB stars (Figure 2). This would reveal whether these concentrated PMS stars are younger than the more widely distributed PMS stars.

6. Conclusion

This paper introduces a new high-resolution X-ray mosaic of the W3 star forming complex, a Large Project of the *Chandra X-ray Observatory*. A rich population of ~ 1300 young stars is imaged and the three well-known regions of high-mass star formation are shown to have very different populations of low mass stars: W3 Main is a large, rich, nearly spherical cluster; W3(OH) lies in an elongated group of sparse stellar clumps; and W3 North is an isolated O star without low-mass companions. Suggestions of these differences were inferred from earlier infrared studies, but they are more apparent here because the X-ray selection has the advantage of low contamination by the Galactic field population or diffuse interstellar emission, high penetration into molecular environments, and little bias towards stars with massive protoplanetary disks.

We emerge from this study with an improved view of star formation in the region. The W3(OH) structures are consistent with collect-and-collapse triggering process caused

by shocks from the older IC 1795 cluster, as previously suggested. The W3 Main cluster, however, does not show the elongated and patchy structure of a recently triggered star cluster and appears to have formed in an earlier episode. Its PMS population strongly resembles those seen in other *Chandra* studies of massive star-forming regions such as those ionizing the Orion, M 17 and Rosette Nebulae. A major difference is that the individual HII regions in these other clusters have already merged into a large blister and dispersed their natal clouds. In contrast, the W3 Main OB stars are very recently formed with small individual HII regions still embedded in a dense, clumpy molecular medium. Star formation in W3 has proceeded in a prolonged fashion, and apparently with a time-dependent Initial Mass Function. The OB stars exciting the hypercompact and ultracompact HII regions at the center of W3 Main formed more recently than the hundreds of X-ray emitting PMS stars distributed over several parsecs. W3 Main thus becomes a critical testbed for theories of rich cluster formation.

We thank Bruce Elmegreen (IBM) and our colleagues at Penn State – Patrick Broos, Gordon Garmire, Kostantin Getman, Masahiro Tsujimoto, and Junfeng Wang – for thoughtful discussions. Patrick Broos and Junfeng Wang additionally provided technical assistance. This work was supported by the *Chandra* General Observer grant G05-6143X (PI Townsley) and by the ACIS instrument team contract SV4-74018 (PI Garmire), both issued by the *Chandra X-ray Observatory* Center, which is operated by the Smithsonian Astrophysical Observatory for and on behalf of NASA under contract NAS8-03060.

Facilities: CXO (ACIS)

Chandra ObsID 446 Chandra ObsID 611 Chandra ObsID 5889 Chandra ObsID 5890
Chandra ObsID 5891 Chandra ObsID 6335 Chandra ObsID 6348

REFERENCES

- Adams, M. T., Strom, K. M., & Strom, S. E. 1983, *ApJS*, 53, 893
- Ballantyne, D. R., Kerton, C. R., & Martin, P. G. 2000, *ApJ*, 539, 283
- Benjamin, R. A., et al. 2005, *ApJ*, 630, L149
- Bonnell, I. A., Bate, M. R., & Zinnecker, H. 1998, *MNRAS*, 298, 93
- Bonnell, I. A., & Clarke, C. J. 1999, *MNRAS*, 309, 461
- Bonnell, I. A., Larson, R. B., & Zinnecker, H. 2007, *Protostars and Planets V*, 149

- Broos, P. S., Getman, K. V., Townsley, L. K., Feigelson, E. D., Wang, J., Garmire, G. P., Jiang, Z. & Tsuboi, Y. 2007, *ApJ*, 169, 353
- Carpenter, J. M., Heyer, M. H., & Snell, R. L. 2000, *ApJS*, 130, 381
- Cesaroni, R., Galli, D., Lodato, G., Walmsley, C. M., & Zhang, Q. 2007, *Protostars and Planets V*, 197
- Chen, H.-R., Welch, W. J., Wilner, D. J., & Sutton, E. C. 2006, *ApJ*, 639, 975
- Dale, J. E., Bonnell, I. A., & Whitworth, A. P. 2007, *MNRAS*, 375, 1291
- de Wit, W. J., Testi, L., Palla, F., & Zinnecker, H. 2005, *A&A*, 437, 247
- DeGioia-Eastwood, K., Throop, H., Walker, G., & Cudworth, K. M. 2001, *ApJ*, 549, 578
- Deharveng, L., Lefloch, B., Massi, F., Brand, J., Kurtz, S., Zavagno, A., & Caplan, J. 2006, *A&A*, 458, 191
- Doom, C., de Greve, J. P., & de Loore, C. 1985, *ApJ*, 290, 185
- Dreher, J. W., & Welch, W. J. 1981, *ApJ*, 245, 857
- Ebeling, H., White, D. A., & Rangarajan, F. V. N. 2006, *MNRAS*, 368, 65
- Elmegreen, B. G., & Lada, C. J. 1977, *ApJ*, 214, 725
- Elmegreen, B. G. 2007, *ApJ*, in press (arXiv:0707.2252)
- Feigelson, E. D., & Montmerle, T. 1999, *ARA&A*, 37, 363
- Feigelson, E. D., Getman, K., Townsley, L., Garmire, G., Preibisch, T., Grosso, N., Montmerle, T., Muench, A. & McCaughrean, M. 2005, *ApJS*, 160, 379
- Feigelson, E., Townsley, L., Güdel, M., & Stassun, K. 2007, in *Protostars and Planets V*, B. Reipurth et al. (eds.), Tucson:Univ. Arizona Press, 313
- Franco, J., García-Segura, G., Kurtz, S. E., & Arthur, S. J. 2007, *ApJ*, 660, 1296
- Freeman, P. E., Kashyap, V., Rosner, R., & Lamb, D. Q. 2002, *ApJS*, 138, 185
- Getman, K. V., Feigelson, E. D., Townsley, L., Bally, J., Lada, C. J., & Reipurth, B. 2002, *ApJ*, 575, 354
- Getman, K. V., et al. 2005, *ApJS*, 160, 319

- Getman, K. V., Feigelson, E. D., Townsley, L., Broos, P., Garmire, G., & Tsujimoto, M. 2006, ApJS, 163, 306
- Getman, K. V., Feigelson, E. D., Garmire, G., Broos, P. & Wang, J., 2007, ApJ, 654, 316
- Güdel, M. et al. 2007, A&A, in press (astro-ph/0609160)
- Hachisuka, K., et al. 2006, ApJ, 645, 337
- Harvey, P., Merin, B., Huard, T. L., Rebull, L. M., Chapman, N., Evans, N. J., & Myers, P. C. 2007, ApJ, 663, 1149
- Herbst, W., & Miller, D. P. 1982, AJ, 87, 1478
- Hofner, P., Delgado, H., Whitney, B., Churchwell, E., & Linz, H. 2002, ApJ, 579, L95
- Kawamura, J. H., & Masson, C. R. 1998, ApJ, 509, 270
- Kim, S.-J., Kim, H.-D., Lee, Y., Minh, Y. C., Balasubramanyam, R., Burton, M. G., Millar, T. J., & Lee, D.-W. 2006, ApJS, 162, 161
- Krumholz, M. R., & Tan, J. C. 2007, ApJ, 654, 304
- Lada, C. J., Elmegreen, B. G., Cong, H.-I., & Thaddeus, P. 1978, ApJ, 226, L39
- Larson, R. B. 2007, Rept. Prog. Phys. 70, 337
- Li, Z.-Y., & Nakamura, F. 2004, ApJ, 609, L83
- Li, Z.-Y., & Nakamura, F. 2006, ApJ, 640, L187
- McMillan, S. L. W., Vesperini, E., & Portegies Zwart, S. F. 2007, ApJ, 655, L45
- Megeath, S. T., Herter, T., Beichman, C., Gautier, N., Hester, J. J., Rayner, J., & Shupe, D. 1996, A&A, 307, 775
- Megeath, S. T., Wilson, T. L., & Corbin, M. R. 2005, ApJ, 622, L141
- Megeath, S. T., Townsley, L., Oey, M. S., & Tiefertunk, A. R. 2007, in *Handbook of Star Forming Regions*, B. Reipurth (ed.), San Francisco: Astro. Soc. Pacific, in press
- Moore, T. J. T, Bretherton, D., Fujiyoshi, T, Ridge, N., Allsopp, J, Hoare, M., Lumsden, S., & Richer, J. 2007, MNRAS, 379, 663
- O'dell, C. R. 1998, AJ, 115, 263

- Oey, M. S., Watson, A. M., Kern, K., & Walth, G. L. 2005, *AJ*, 129, 393
- Ogura, K., Chauhan, N., Pandey, A. K., Bhatt, B. C., Ojha, D. & Itoh, Y. 2007, *PASJ*, 59, 199
- Ogura, K., & Ishida, K. 1976, *PASJ*, 28, 651
- Ojha, D. K., et al. 2004, *ApJ*, 608, 797
- Palla, F., & Stahler, S. W. 2000, *ApJ*, 540, 255
- Povich, M. S., et al. 2007, *ApJ*, 660, 346
- Preibisch, T., & Feigelson, E. D. 2005, *ApJS*, 160, 390
- Preibisch, T., et al. 2005, *ApJS*, 160, 401
- Reid, M. J., Haschick, A. D., Burke, B. F., Moran, J. M., Johnston, K. J., & Swenson, G. W., Jr. 1980, *ApJ*, 239, 89
- Ruch, G. T., Jones, T. J., Woodward, C. E., Polomski, E. F., Gehrz, R. D., & Megeath, S. T. 2007, *ApJ*, 654, 338
- Shull, J. M., & Saken, J. M. 1995, *ApJ*, 444, 663
- Skinner, S. L., Simmons, A. E., Audard, M., Güdel, M. 2007, *ApJ*, 658, 1144
- Sugitani, K., Tamura, M., & Ogura, K. 1995, *ApJ*, 455, L39
- Tan, J. C., Krumholz, M. R., & McKee, C. F. 2006, *ApJ*, 641, L121
- Thronson, H. A., Jr., Schwartz, P. R., Smith, H. A., Lada, C. J., Glaccum, W., & Harper, D. A. 1984, *ApJ*, 284, 597
- Thronson, H. A., Jr., Lada, C. J., & Hewagama, T. 1985, *ApJ*, 297, 662
- Tieftrunk, A. R., Gaume, R. A., Claussen, M. J., Wilson, T. L., & Johnston, K. J. 1997, *A&A*, 318, 931
- Tieftrunk, A. R., Megeath, S. T., Wilson, T. L., & Rayner, J. T. 1998, *A&A*, 336, 991
- Townsley, L. K., Broos, P. S., Nousek, J. A., & Garmire, G. P. 2001, *Nuclear Instr. & Methods*, 486, 751
- Townsley, L. K., Feigelson, E. D., Montmerle, T., Broos, P. S., Chu, Y.-H., & Garmire, G. P. 2003, *ApJ*, 593, 874

- Townsley, L. K. 2006, in "Massive Stars: From Pop III and GRBs to the Milky Way," ed. M. Livio, in press (astro-ph/0608173)
- Townsley, L. K., Broos, P. S., Feigelson, E. D., Garmire, G. P., & Getman, K. V. 2006, *AJ*, 131, 2164
- Tsujimoto, M., et al. 2007, *ApJ*, 665, 719
- Turner, J. L., & Welch, W. J. 1984, *ApJ*, 287, L81
- van der Tak, F. F. S., Tuthill, P. G., & Danchi, W. C. 2005, *A&A*, 431, 993
- van der Werf, P. P., & Goss, W. M. 1990, *A&A*, 238, 296
- Wang, J., Townsley, L. K., Feigelson, E. D., Getman, K. V., Broos, P. S., Garmire, G. P., & Tsujimoto, M. 2007a, *ApJS*, 168, 100
- Wang, J., Townsley, L. K., Feigelson, E. F., Broos, P. S., Getman, K. V., Roman-Zuniga, C. & Lada, E. 2007b, submitted for publication
- Wang, J., Townsley, L. K., Feigelson, E. F., Getman, K. V., Broos, P. S., Roman-Zuniga, C. & Lada, E. 2007c, in preparation
- Weisskopf, M. C., Brinkman, B., Canizares, C., Garmire, G., Murray, S., & Van Speybroeck, L. P. 2002, *PASP*, 114, 1
- Whitworth, A. P., Bhattal, A. S., Chapman, S. J., Disney, M. J., & Turner, J. A. 1994, *A&A*, 290, 421
- Wyrowski, F., Schilke, P., Walmsley, C. M., & Menten, K. M. 1999, *ApJ*, 514, L43
- Xu, Y., Reid, M. J., Zheng, X. W., & Menten, K. M. 2006, *Science*, 311, 54
- Zacharias, N., Monet, D. G., Levine, S. E., Urban, S. E., Gaume, R., & Wycoff, G. L. 2005, *VizieR Online Data Catalog*, 1297, 0
- Zavagno, A., Deharveng, L., Comerón, F., Brand, J., Massi, F., Caplan, J., & Russeil, D. 2006, *A&A*, 446, 171

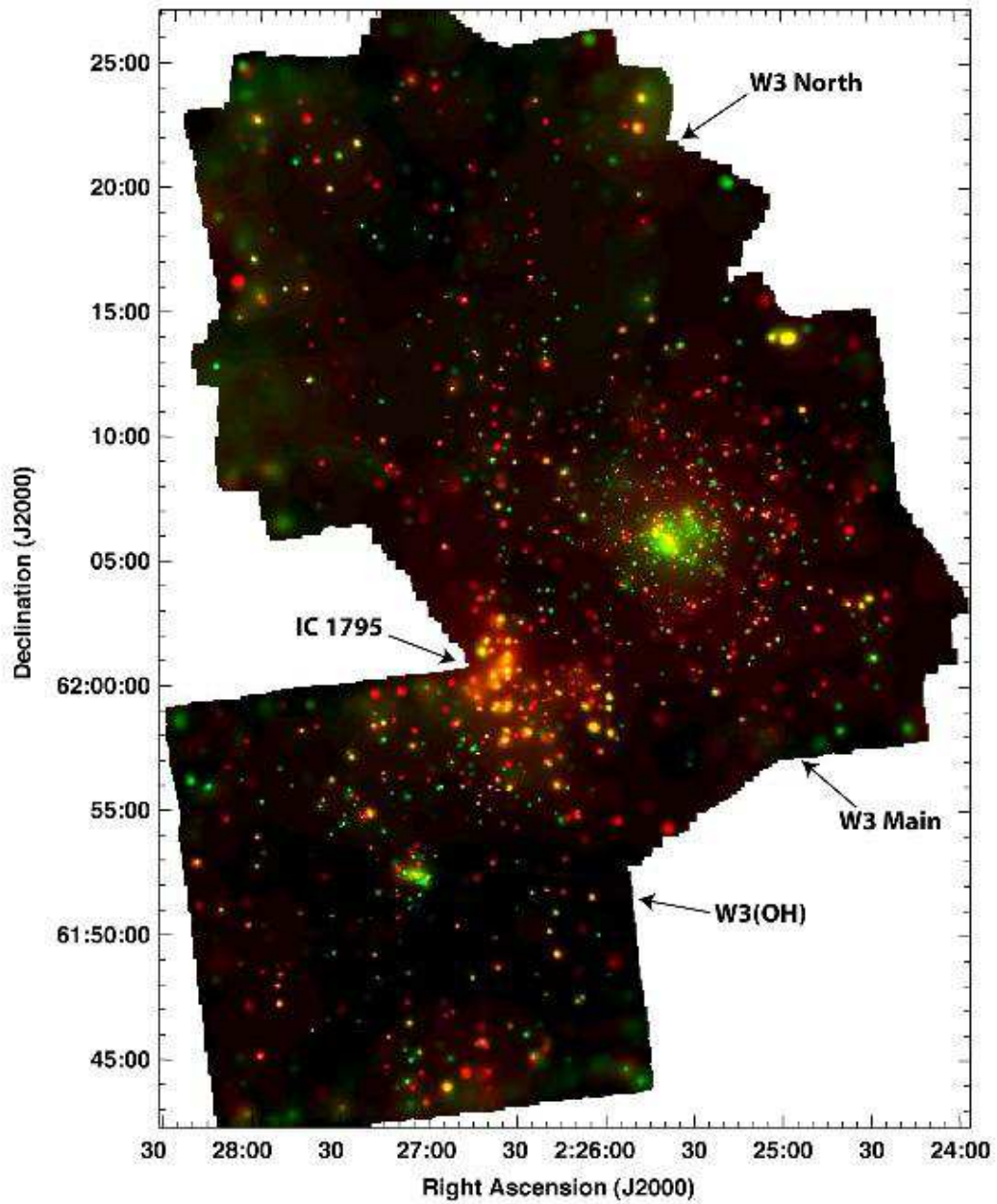


Fig. 1.— A smoothed X-ray mosaic of W3 from the *Chandra*/ACIS data where red intensity is scaled to the 0.5–2 keV emission and green is scaled to 2–7 keV emission. The ~ 800 arcmin² mosaic includes W3 North, W3 Main, part of the older cluster IC 1795, W3(OH), and two small IR clusters located northeast of W3(OH). Each of the seven ACIS-I pointings covers $17' \times 17'$.

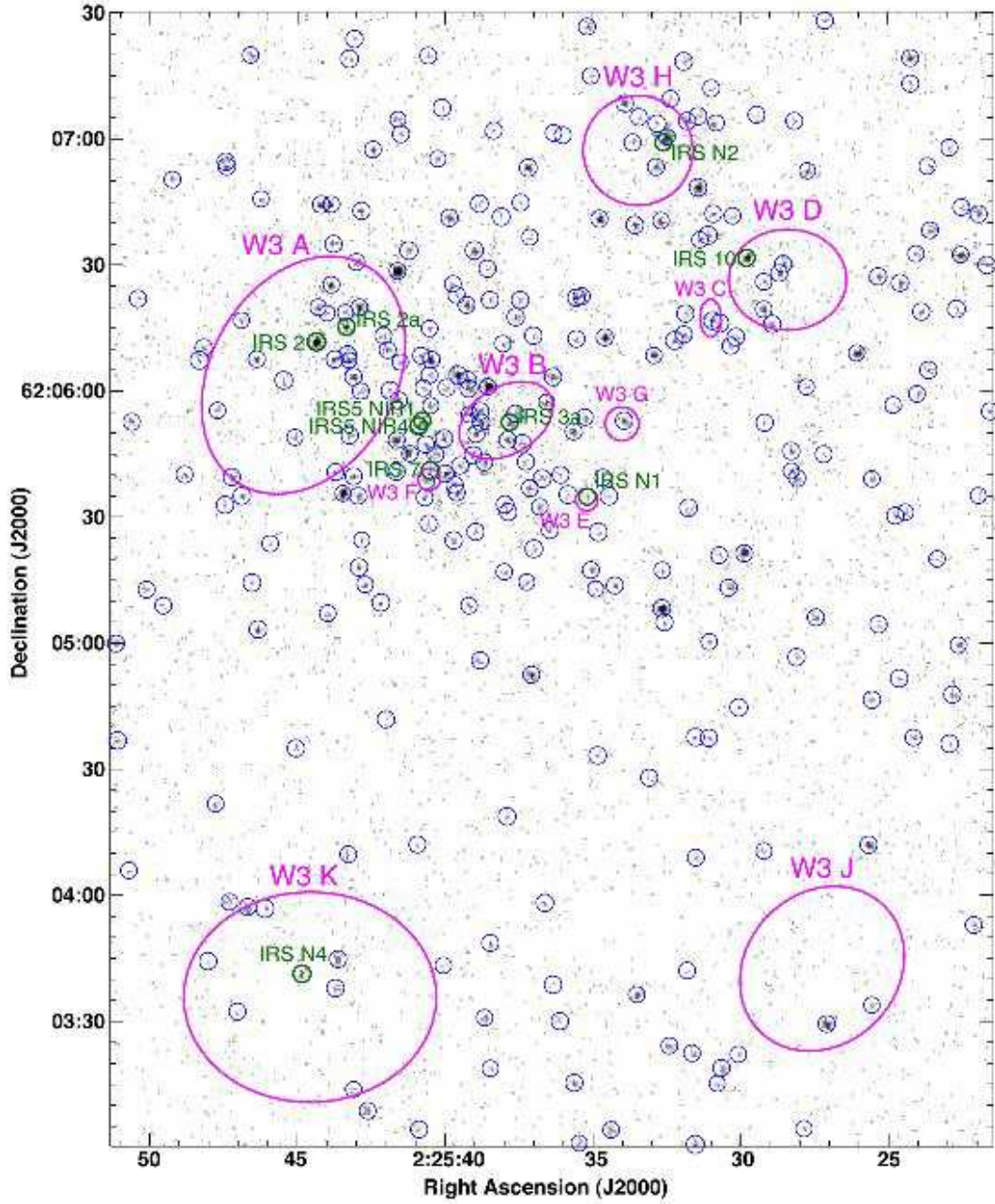


Fig. 2.— *Chandra* ACIS image of W3 Main ($3.5' \times 4.5'$, 2.0×2.6 pc) showing individual photon events. Well-studied radio HII regions (magenta ellipses) and bright infrared sources (green circles) are labeled.

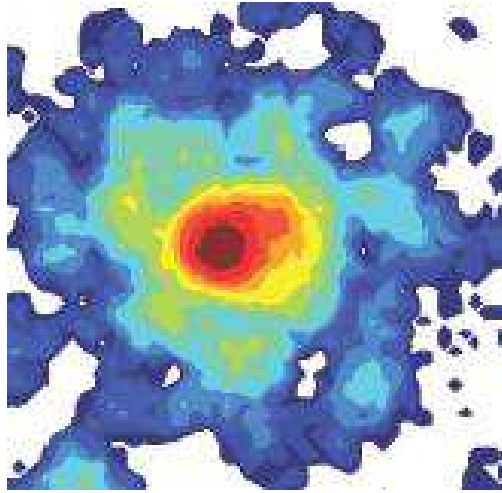


Fig. 3.— Large-scale distribution of X-ray sources in W3 Main ($10'$, 5.8 pc), smoothed with a $30''$ (0.3 pc) kernel. Colors represent logarithmic range of source surface density from 0.03 (dark blue) to 10 (brown) stars arcmin^{-2} .

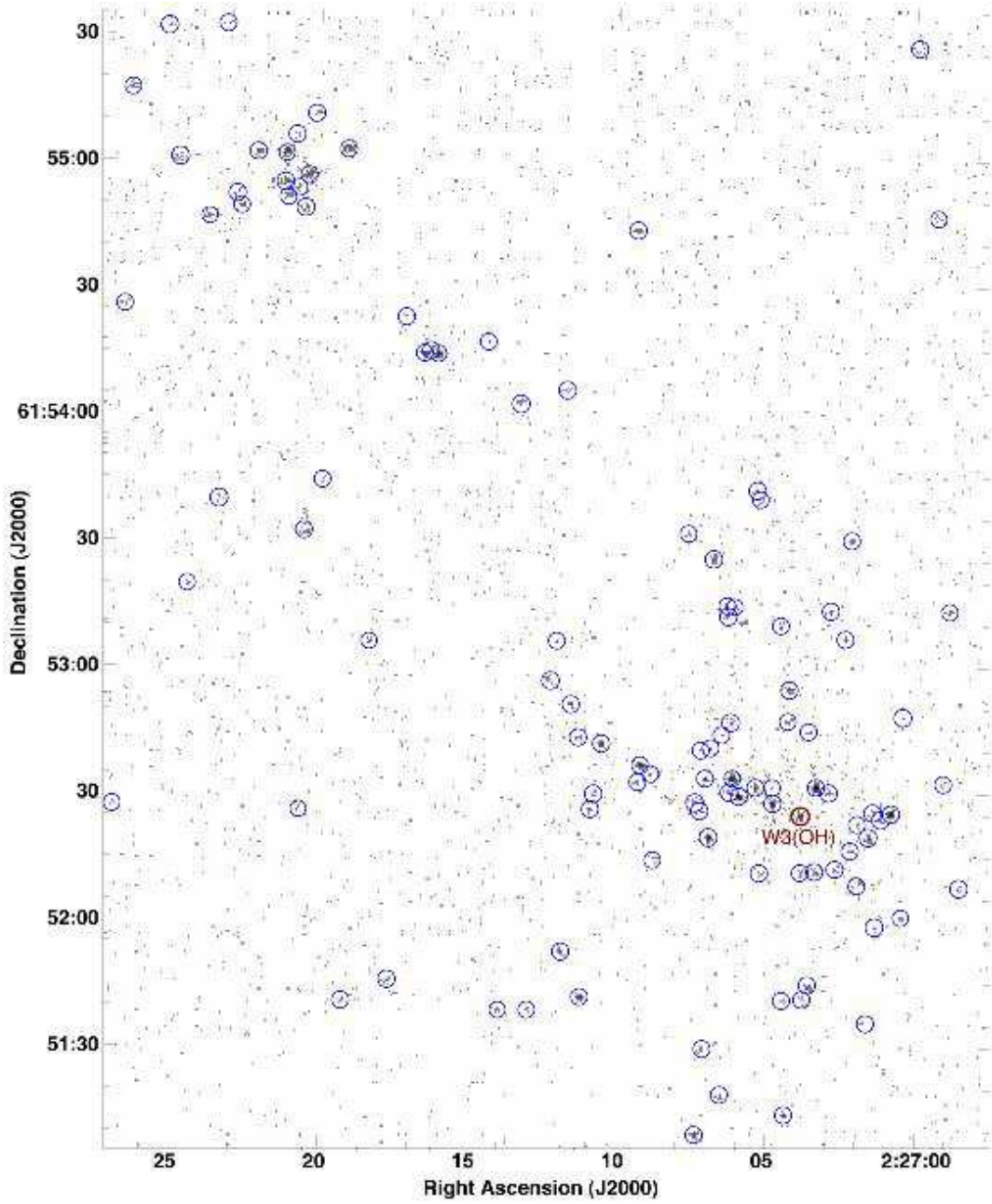


Fig. 4.— ACIS image of the W3(OH) cluster and two small IR clusters to its northeast ($3.5' \times 4.5'$, 2.0×2.6 pc). The X-ray source at the center of the UCHII region W3(OH) is marked.

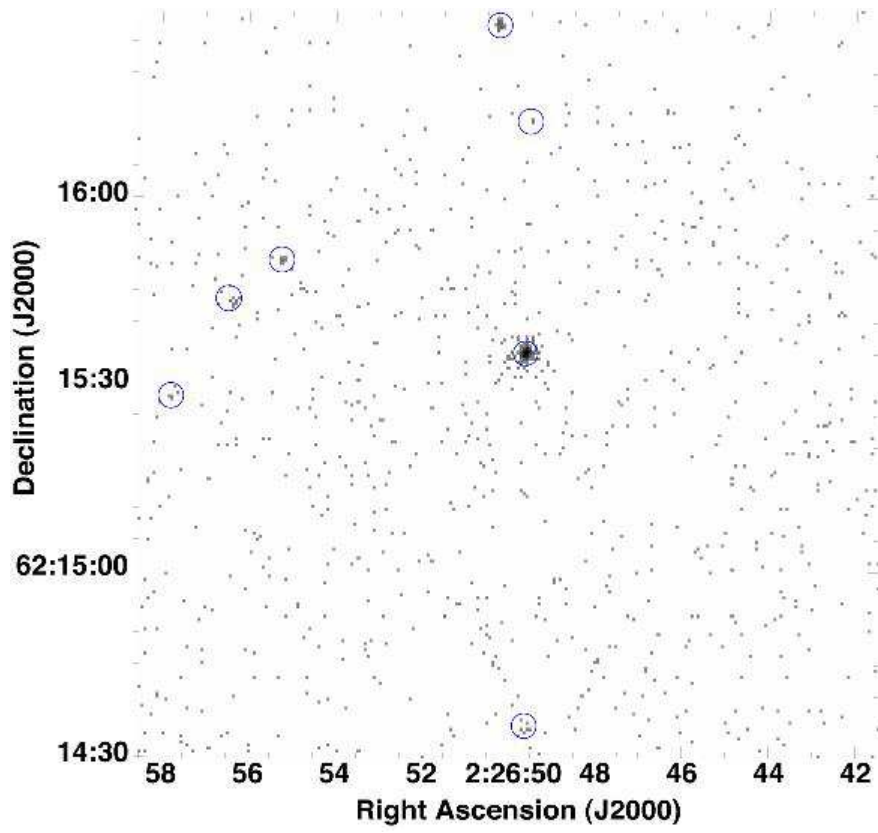


Fig. 5.— *Chandra* image of W3 North ($2'$, 1.2 pc). The bright X-ray source at field center is the isolated O6 star.